DOI: 10.26599/FSHW.2026.9251183

Contents lists available at SciOpen

Food Science and Human Wellness

journal homepage: https://www.sciopen.com/journal/2097-0765

China Food Publishing Co.

Genomic Insights and Phenotypic Assessment of *Lactobacillus rhamnosus* GYX-9: Unraveling Its Probiotic Potential in Ameliorating Obesity-Associated Metabolic Disorders

Kailun Dong[a], Donghu Tan[a], Tianjing Long[a], Weimei Kong[a], Yijin Zhang[a], Haibo Luo[a], Xiaoqun Zeng[b], Zhen Wu[b], Mingxuan Tao[a], Daodong Pan[b], Yuxing Guo[a*]

[a] *Department of Food Science and Technology, School of Food Science and Pharmaceutical Engineering, Nanjing Normal University, Nanjing, 210023, Jiangsu, China*

[b] *College of Food and Pharmaceutical Sciences, Ningbo University, Ningbo, 315211, Zhejiang, China*

ABSTRACT: To prevent or improve obesity and metabolic diseases caused by long-term high-fat diets (HFD), this study screened probiotic strains based on their probiotic properties predicted from their whole genomes and validated their probiotic functions through in vitro and *in vivo* experiments. In the preliminary phase, *Lactobacillus rhamnosus* GYX-9, a strain with strong adhesion properties, was isolated from the gut of healthy infants. Functional annotation revealed high gene abundance related to processes such as the tricarboxylic acid cycle and lipid metabolism. Notably, genes encoding aldehyde dehydrogenase/alcohol dehydrogenase and acetyl-CoA acetyltransferase played significant roles in lipid reduction. Furthermore, this strain possesses genes involved in the acetate synthesis pathway, such as *ackA* and *pta*. *In vitro* validation demonstrated its strong ability to inhibit α-amylase and lower cholesterol. Intervention with this strain in high-fat mice reduced weight gain; increased high-density lipoprotein cholesterol (HDL-C) levels by 155.02%; enhanced catalase (CAT) antioxidant enzyme activity in the liver by 35.5%; and decreased colonic interleukin-1β (IL-1β) by 52.65%; and increased interleukin-10 (IL-10) levels to (170.55 ± 36.34) pg/mL.. The relative abundance of *Bifidobacterium* and *Romboutsia* increased, while *Ileibacterium* and *Desulfovibrio* decreased. These findings provide important theoretical and practical references for developing safe and effective obesity intervention strategies.

Keywords: *Lactobacillus rhamnosus;* genome; lipid-lowering; metabolism

1. Introduction

As living standards improve, people increasingly seek to enhance the taste of their food. However, delicious flavors often come at the cost of high sugar and fat content, leading to a rapid rise in obesity worldwide. Based on current trends, by 2030 approximately 50% of the adult population will be affected by overweight or obesity[1]. Obesity is often accompanied by various health issues, such as cardiovascular disease, diabetes, and others[2].

***Corresponding author**
guoyuxing1981@163.com

Received 7 December 2025
Received in revised from 19 January 2026
Accepted 9 February 2026

Currently, there are limited pharmacological options available for obesity treatment, with orlistat and phentermine being the primary drugs approved internationally. However, orlistat can cause allergic reactions, liver damage, and kidney damage[3]. Therefore, identifying safe and effective alternative intervention strategies has become a key research focus in this field. Probiotic interventions are recognized as safe and free of side effects. Currently, lactobacilli such as *Lactobacillus fermentus* CQPC07[4], *Lactobacillus plantarum* Lp3[5], *Lactobacillus paracasei* K56[6], *Lactobacillus salivarius* ADM14[7], and *Bifidobacterium* spp.[8] have lipid-lowering effects. Mixed lactic acid bacteria (LAB) improve indicators associated with high-fat diets by regulating the gut microbiota structure, thereby inhibiting obesity[9]. Viable *Lactobacillus paracasei* K56 and its surface proteins -+effectively reduce fat synthesis and improve lipid metabolism through the PPAR-γ/CEBP-α-mediated lipid synthesis pathway[6].

Surface proteins constitute a vital component of the extracellular structure of *Lactobacillus* cells, playing a significant role in the adhesion of LAB to hosts. They are categorized into surface layer proteins, LPXTG proteins, and moonlighting proteins[10]. S-layer proteins exhibit unique self-assembly properties, enabling interactions with extracellular matrix proteins such as laminin, fibronectin, and desmin. LPXTG motif proteins enhance bacterial adhesion to intestinal cells by increasing surface hydrophobicity and promoting self-aggregation. Moonlighting proteins perform diverse roles, contributing not only to adhesion but also to other physiological processes. Previous studies have identified several surface proteins in *L. rhamnosus*, including *L. rhamnosus* possesses surface proteins such as S-layer proteins[11], enolase, Glyceraldehyde-3-phosphate dehydrogenase (GAPDH), and lactate dehydrogenase (LDH)[12], which facilitate adhesion to the intestinal mucosa and contribute to the bacterium's probiotic potential.

LAB is an effective approach for improving obesity. Exploring highly effective lipid-lowering LAB is of great significance for expanding the development of probiotic lipid-lowering products. The probiotic properties of *L. rhamnosus* are increasingly recognized, including regulating intestinal microbiota[14, 15], enhancing immune function[16] and exhibiting antioxidant properties[17]. These properties enhance the potential of *L. rhamnosus* to reduce blood lipids.

Traditional methods for assessing the functional activity of a lactobacillus strain require time-consuming individual testing. Whole-genome sequencing technology enables in-depth analysis of *Lactobacillus* metabolic mechanisms, genetic information, and physiological functions, providing a crucial basis for screening strains with superior probiotic properties[18]. The genes involved in the basic L-glutamine metabolism related to blood sugar and lipid reduction in the genome of *Lactobacillus plantarum* 84-3 include *Abc.glnl.A* and *gtnA*[19]. Few studies have reported the prediction of *L. rhamnosus* functional activity from a probiotic whole-genome perspective and its *in vivo* validation. The present study aimed to understand the genomic characteristics of *L. rhamnosus* GYX-9 through whole-genome sequencing, assess its probiotic potential and genetic features, and investigate its lipid-lowering activity by examining changes in obesity indicators and gut microbiota in high-fat mice following *L. rhamnosus* GYX-9 intervention.

2. Materials and methods

2.1 Materials

Man-Rogosa-Sharpe (MRS) broth was purchased from Qingdao Haibo Biotechnology Co., Ltd. (Qingdao, China). *L. rhamnosus* GYX-9 was isolated from the intestines of healthy infants and deposited at the China General Microbial Culture Collection Center (CGMCC) with the deposit number No. 30946. Bovine bile salts and cholesterol were acquired from Shanghai Yuanye Biotechnology Co., Ltd. (Shanghai, China). Antibiotic susceptibility disks were purchased from Hangzhou Microbiology Reagent Co., Ltd. (Hangzhou, China). Blood agar plates were purchased from Changde Beekman Biotechnology Co. (Changde, China). Various enzyme activity assay kits were supplied by Beijing Solepol Technology Co., Ltd. (Beijing, China). Various mouse ELISA kits were provided by Shanghai Thrive Color Biotechnology Co. High-fat mice were provided by Nanjing Baiwuorui Pharmaceutical Research Institute (Nanjing, China).

2.2 Characteristics Study of L. rhamnosus GYX-9

2.2.1 Determination of inhibition rate of α-amylase of L. rhamnosus GYX-9

Refer to Houda Ben-Miled's method[20], 1 mL of reaction mixture in 0.04 mol/L phosphate buffer (pH5.8), containing 100 μL of an overnight culture and 500 μL of 1% soluble starch used as substrate, was prepared and pre-incubated at 37℃ for 3 min. Thereafter, 100 μL of α-amylase solution 0.5 mg/mL were added. Then, the mixture was incubated at 25℃ for 10 min. The reaction was stopped by adding 100 μL of 0.1 M HCl. Next, 100 μL of the mixture was reacted with 1.5 mL 3% Liodine solution for 30 min at room temperature. Finally, the absorbance was measured at 540 nm. The α-amylase inhibition rate was calculated according to the following equation:

$$\alpha - \text{Amylase inhibition rate}(\%) = \left(1 - {(\text{Abs}_{\text{Sanmple}} - \text{Abs}_{\text{blank}})}/{\text{Abs}_{\text{control}}}\right) \times 100 \quad (1)$$

where $\text{Abs}_{\text{sample}}$, $\text{Abs}_{\text{control}}$ and $\text{Abs}_{\text{blank}}$ represent the absorbance of the experimental sample, the solution without bacteria and the mixture without the substrate.

2.2.2 Determination of cholesterol-lowering ability of L. rhamnosus GYX-9

Preparation of cholesterol-enriched MRS medium (MRS-CHOL medium): Cholesterol (0.1 g), bovine bile salts (0.2 g), and sucrose ester (0.1 g) were homogenized in 1 mL Tween-80, followed by the addition of 5 mL glacial acetic acid with heating at 60℃ to form a micellar solution. The mixture was sonicated and sterilized (121℃, 15 min).

LAB was inoculated at a volume fraction of 5.0% into MRS-CHOL medium incubated at 37℃ for 24 h. After cultivation, cells were harvested by centrifuging (8,000×*g*, 10 min, 4 °C) and the supernatant was collected. The cholesterol contents in the supernatant and uninoculated medium were determined using the o-phthalaldehyde method described by Rudel and Morris[21]. The cholesterol degradation rate is calculated as follows:

$$Cholesterol\ \ Degradation\ \ Rate(\%) = {(C - A)}/{C} \times 100 \quad (2)$$

Where: C = cholesterol concentration in the control group, A = cholesterol concentration in the test strain.

2.2.3 Adhesion of L. rhamnosus GYX-9 to Collagen and Mucin

Cultivate 50 mL of *L. rhamnosus* GYX-9, washed twice with 0.01 M phosphate-buffered saline (PBS, pH7.4, Gibco) and add 750 μL pH2, 5 mol/L lithium chloride (LiCl, Sangon Biotech Co., Ltd., China) on ice for 20 min, followed by centrifugation at 6,000×*g* for 20 min at 4℃. The supernatant was discarded, and pellets were resuspended in sterile PBS to generate surface proteins extracted bacterial suspensions.

Refer to the method of Wu et al[10]. Mucin and collagen (Sigma-Aldrich, St. Louis, MO, USA; 5 mg/mL each) were immobilized in 12-well plates (2 mL/well) by overnight fixation at 4°C. After washing with PBS, *L. rhamnosus* GYX-9 was added and incubated at 37℃ for 2 h. Unattached bacteria were removed by PBS washing, and adherent cells were released by treatment with 0.05% Triton X-100 at 37°C for 20 min. Live bacterial counts were determined by inoculating onto MRS agar plates, and the adhesion rate was calculated using the following formula:

$$Adhesion\ rate\ (\%) = {}^{lgN_1}/_{lgN_0} \times 100 \quad (3)$$

Where N_0 is the number of live bacteria in the bacterial solution before adhesion/(CFU/mL); N_1 is the number of live bacteria adhered to the protein/(CFU/mL).

2.2.4 Protein Profiling by SDS-PAGE

The extracted total surface proteins from the probiotic strains were characterized for their size and type using SDS-PAGE (10% gel) protein profiling following the standard protocol[22]. Analyzing electrophoresis patterns using a gel imager.

2.2.5 L. rhamnosus GYX-9 antibiotic resistance

The drug susceptibility of *L. rhamnosus* to antibiotics was determined by the Kirby-Bauer disk diffusion method[23]. Antibiotic types for disk diffusion susceptibility testing (Hangzhou Microbial Reagents Co., Ltd.) include: penicillin、 Cotrimoxazole、 ampicillin、 cefazolin、 amikacin、 gentamicin、 norfloxacin、 ciprofloxacin、erythromycin and chloramphenicol. Concentration: 30 μg/disc. *L. rhamnosus* GYX-9 cultures (1×10^8 CFU/mL) were spread on MRS agar, antibiotic discs were applied, and plates were incubated at 37℃ for 48 h. Inhibition zone diameters were measured.

2.3 Genomic DNA extraction and sequencing of L. rhamnosus GYX-9

L. rhamnosus GYX-9 was cultured at 37℃ for 12 h, and genomic DNA was extracted for sequencing (project ID: SLT). Whole genome sequencing was performed using Illumina HiSeq and PacBio platforms (Shanghai, China). Genomic DNA was sheared into ~ 10 kb fragments, followed by library construction and paired-end sequencing.

2.4 Genome assembly, prediction and functional annotation

Illumina reads were quality-trimmed and assembled using SOAPdenovo 2. Genomic islands were predicted with IslandPath-DIMOB, virulence and antibiotic resistance genes were analyzed with VFDB, and functional annotation was performed against GO, COG, KEGG, and CAZy databases.

2.5 Animal experiments

All experimental protocols were approved by the Institutional Animal Care and Use Committee of Nanjing Normal University (SYXK(Su) 2015-0028). Eighty male C57BL/6J mice, aged six weeks, were obtained from Aniphe Biolaboratory Inc. (Jiangsu, China). The mice were housed under controlled conditions (22 ± 2℃, 40%-60% humidity, 12 h light/dark cycle) with ad libitum access to feed and water. After one week of acclimatization, the mice were randomly divided into a normal diet (Control) group (n = 10) and an HFD (Model) group (n = 35), the high-fat feed contains lard and soybean oil, with a fat content of 35% and fat providing 60% of total calories. It took 9 weeks to establish the high-fat model.

The Control group was fed a standard rodent chow, while the Model group received a high-fat diet (D12492, Research Diets Inc., USA). By week ten, the HFD-fed mice were subdivided into three groups (n = 10) based on body weight, with specific diets in Table S1. The orlistat group serves as a positive group for comparison. The feeding lasted six weeks, during which the mice were weighed weekly, and their general health conditions were monitored.

At the end of the feeding period, the mice were fasted for 12 h before euthanasia via cervical dislocation under anesthesia. Blood samples, liver tissues, fecal samples, and epididymis were immediately collected and stored at -80℃ for further analysis for a maximum of 8 weeks.

2.6 Measurement of insulin sensitivity in mice

After 12 h fasting, mice received 2 g/kg glucose by oral gavage. Blood glucose was measured at 0, 15, 30, 60, 90, and 120 min. Serum insulin was quantified by ELISA.

2.7 Biochemical analysis in the serum of mice

Serum was obtained by centrifuging blood at 3,000×*g* for 15 min at 4℃. Total cholesterol (TC), low-density lipoprotein (LDL-C), triglyceride (TG), and high-density lipoprotein (HDL-C) were measured by adding 2.5 μL of serum to the assay reagents and following the protocol provided by the assay kits (Nanjing Jiancheng Bioengineering Institute, Nanjing, China). Similarly, serum levels of adiponectin, leptin, and insulin were assessed according to the instructions of commercially available ELISA kits (Beijing Solarbio Science & Technology Co., Ltd., Beijing, China).

2.8 Determination of oxidative stress indicators and free fatty acids in mouse liver

Liver samples were weighed, diluted in saline (1:9), and homogenized on ice. After centrifugation at 2,500×*g* for 10 min at 4℃, the supernatant was collected for the analysis of FFA, catalase (CAT), superoxide dismutase (SOD), and malondialdehyde (MDA) using commercially available analytical kits (Beijing Solarbio Science & Technology Co., Ltd., Beijing, China) in accordance with the manufacturer's instructions.

2.9 Determination of inflammatory factors in the mouse colon

Proximal colon tissue was weighed and homogenized by adding 19× the volume of saline for 40 s. Following homogenization, the mixture was centrifuged at 3,500×*g* for 15 min at 4℃ to collect the supernatant. Levels of interleukin-1β (IL-1β), interleukin-10 (IL-10), interleukin-6 (IL-6), and tumor necrosis

factor-α (TNF-α) were quantified according to the instructions of commercially available ELISA kits (ZCIBIO Technology Co., Ltd., Shanghai, China).

2.10 Gut microbiota analysis

Total microbial genomic DNA was extracted from fecal samples using the FastPure Feces DNA Isolation Kit (Shanghai Major Yuhua, Shanghai, China) according to the manufacturer's protocol. DNA concentration and purity were assessed with a NanoDrop2000 spectrophotometer (Thermo Fisher Scientific, Waltham, USA), and the integrity was verified via 1.2% agarose gel electrophoresis. The V3-V4 hypervariable regions of the 16S rRNA gene were amplified with primer pairs 338F (5'-ACTCCTACGGGAGGCAGCAG-3') and 806R (5'-GGACTACHVGGGTWTCTAAT-3') by T100 Thermal Cycler PCR thermocycler (BIO-RAD, USA). Purified amplicons were pooled in equimolar amounts and paired-end sequenced on an Illumina PE300 platform (Illumina, San Diego, USA) according to the standard protocols by Majorbio Bio-Pharm Technology Co., Ltd. (Shanghai, China). Raw sequencing data were quality-controlled using fastp (v0.19.6) and merged with FLASH (v1.2.7). The optimized sequences were clustered into operational taxonomic units (OTUs) using UPARSE (v7.1) at 97% similarity. Taxonomic classification was performed with RDP Classifier (v2.11) against the SILVA database (v138) with a confidence threshold of 0.7. Bioinformatic analysis of the gut microbiota was carried out using the Majorbio Cloud platform (https://cloud.majorbio.com).

2.11 Statistical analysis

Experimental data are presented as mean ± standard error of the mean. Data were analyzed using IBM SPSS Statistics 26, and statistical differences were evaluated using one-way ANOVA followed by Duncan's multiple comparison test at $P < 0.05$. GraphPad Prism 8 was used for chart creation.

3. Results

3.1 Probiotic Properties of LAB

Inhibiting α-amylase activity prevents the breakdown of carbohydrates into monosaccharides, subsequently reducing blood glucose levels[24]. Comparing *L. rhamnosus* GYX-9 with *Lactobacillus casei* GYX-1 and *Streptococcus thermophilus* GYX-8 from the laboratory collection, *L. rhamnosus* GYX-9 exhibited an α-amylase inhibitory effect of (78.95 ± 12.42)% (Fig.1A), significantly higher than that of *Limolactobacillus fermentum* and *Lacticaseibacillus casei* isolated by Handana Kumari V. B. et al[25]., which exhibited α-amylase inhibition rates ranging from 20.21% to 56.91%. Studies suggest that lactobacilli may possess cholesterol-lowering effects[26]. Specifically, *L. rhamnosus* GYX-9 showed a cholesterol degradation rate of (69.89 ± 8.61)% (Fig.1B), significantly higher than *Lactobacillus casei* GYX-1 (59.40 ± 8.54)% and and *Streptococcus thermophilus* GYX-8 (61.65 ± 17.62%). It was also significantly higher than *Lactobacillus plantarum* ATCC 43121 (29%)[27]. This may be attributed to the adsorption and coprecipitation of cholesterol by *L. rhamnosus* GYX-9 or the higher BSH enzyme activity[28, 29]. In conclusion, *L. rhamnosus* GYX-9, with its potent α-amylase inhibition and cholesterol-lowering capabilities, holds market potential for application in glucose-lowering and lipid-lowering products.

The adhesion of LAB to the intestinal wall is one of the prerequisites for exerting probiotic effects. Therefore, we compared the adhesion of *L. rhamnosus* GYX-9 with and without surface proteins to collagen and mucin. As can be seen from Table 1, the adhesion rate of *L. rhamnosus* GYX-9 to collagen and mucin was (82.46 ± 1.22)%, (78.06 ± 0.07)%. And the adhesion rate of *L. rhamnosus* GYX-9 to collagen and mucin after removal of surface proteins was reduced to (67.81 ± 0.31)%, (69.85 ± 0.44)%. These results suggest that surface proteins act as adhesion factors, facilitating the intestinal colonization of *Lactobacillus*.

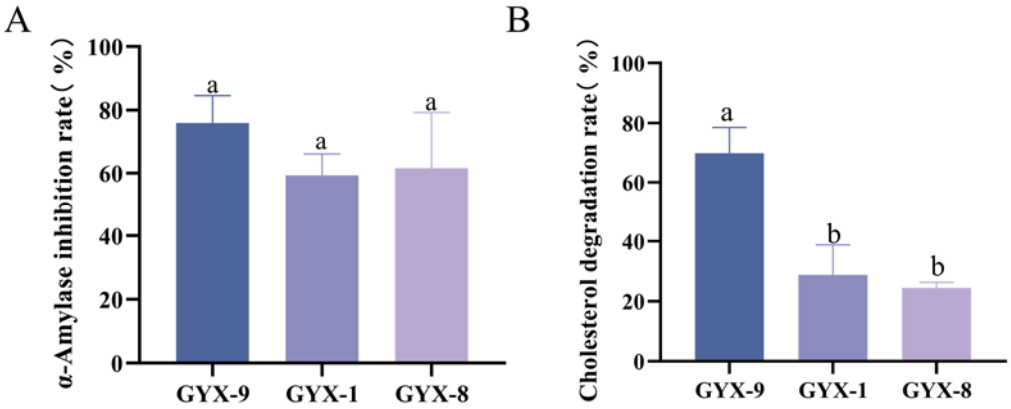

Fig.1 *In vitro* probiotic properties of *L. rhamnosus* GYX-9 (A) α-Amylase Inhibition Rate and (B) Cholesterol degradation rate.

Table 1 Probiotic properties of *L. rhamnosus* GYX-9

	Adhesion to collagen proteins (%)	Adhesion to mucin (%)
L. rhamnosus GYX-9	82.46 ± 1.22	78.77± 0.07
L. rhamnosus GYX-9 with surface proteins removed	67.81 ± 0.32	69.85 ± 0.45

3.2 Surface Protein SDS-PAGE Analysis

As shown in Fig.2, SDS-PAGE analysis of surface proteins from *L. rhamnosus* GYX-9 shows distinct bands at 95 kDa and 41-52 kDa, with an additional band at 52-72 kDa. Based on existing reports and Uniprot database searches, we speculate that the protein at 41-52 kDa may include S-layer proteins (SLP)[30], enolases, and mucus binding factor (MBF) proteins[31]. *L. rhamnosus* Spa has been reported to be associated with intestinal mucus adhesion. The SpaB bacterial protein may possess similar mucus-crosslinking capabilities and potentially function through electrostatic interactions. UniProt lists its molecular weight as 120 kDa. Furthermore, the fimbrial subunit (SpaC) is also implicated in intestinal mucus binding[32], with UniProt reporting a molecular weight of 90 kDa.

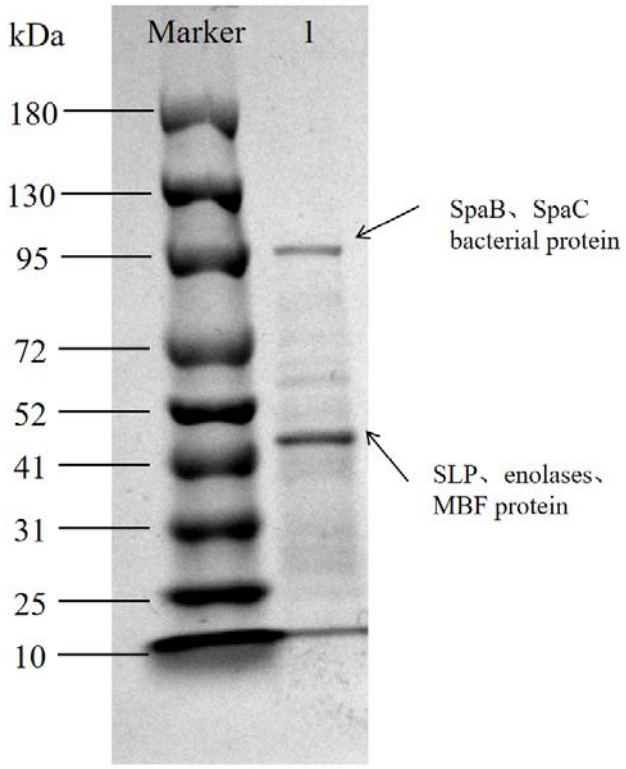

Fig.2 *L. rhamnosus* GYX-9 surface protein SDS-PAGE analysis. Lane 1: *L. rhamnosus* GYX-9 surface proteins

3.3 L. rhamnosus GYX-9 antibiotic resistance

Antibiotic susceptibility serves as a crucial criterion in evaluating the safety profile of microorganisms. A comparison with established reference standards revealed that *L. rhamnosus* GYX-9 demonstrated sensitivity to ampicillin, cefazolin, and chloramphenicol; resistance to penicillin, amikacin, gentamicin, norfloxacin, and cotrimoxazole; and intermediate resistance to ciprofloxacin and erythromycin (Table S2). These results indicate that *L. rhamnosus* GYX-9 is a safe candidate for the development of probiotic preparations.

3.4 Basic characterization and compositional analysis of the whole genome sequence

L. rhamnosus GYX-9 exhibits the highest affinity for *L. rhamnosus* strain GCF_900636965.1. The genome lengths of various *Lactobacillus* species and subspecies typically range between 1.8 and 3.3 Mb[33]. The genome of *L. rhamnosus* GYX-9, the focus of this study, comprises 2,982,036 base pairs (Fig.3) and includes 15 rRNA genes, 59 tRNA genes, and 2,739 coding sequence (CDS) that encode 1,374 proteins, among which 87 are carbohydrate-active enzymes. Similar to most *Lactobacillus* genomes, which typically exhibit a GC content below 50%, *L. rhamnosus* GYX-9 has a GC content of 46.85% (Table S3). This value falls within the normal range and is notably comparable to that of *L. rhamnosus* LS-8 (46.68%)[34].

Genomic islands (GI) contain genes associated with a variety of biological functions. The predicted GIs of *L. rhamnosus* GYX-9 have a total of 14 GI, all belonging to the chromosome, with the shortest GI being 5,314 bp and the longest being 52,677 bp (Table S4.), which is larger than that of other prokaryotic organisms that have been reported[35].

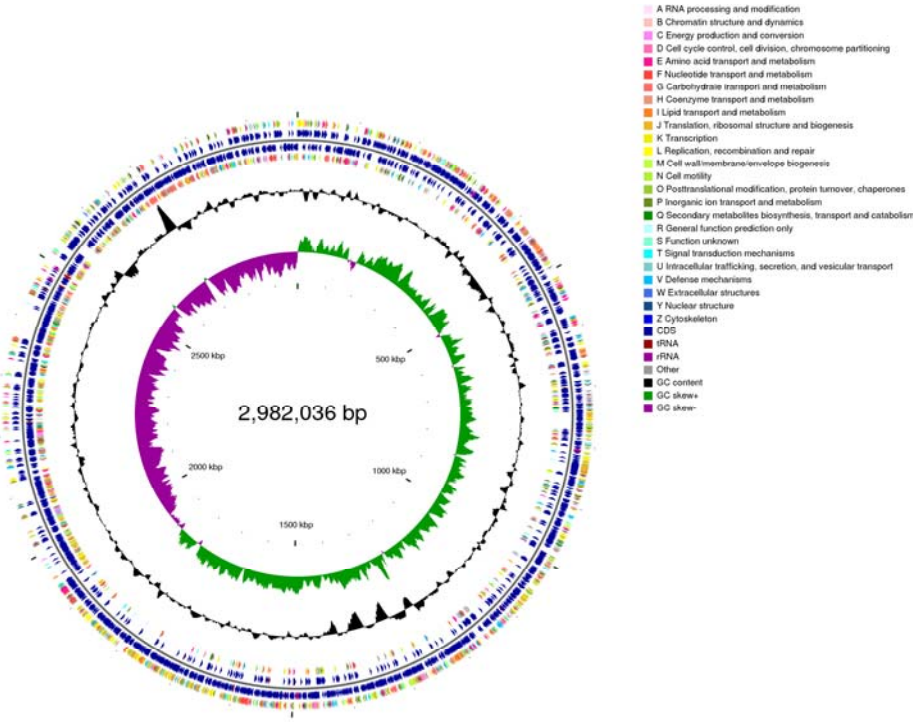

Fig.3 CGView genomic circle map of *L. rhamnosus* GYX-9

Analysis of its pathogenic system shows that *L. rhamnosus* GYX-9 contains 69 genes related to nutritional/metabolic factors, 59 genes related to immune regulation, 36 genes such as exotoxin, and no pathogenic aggressive factors (Fig.4A), which is consistent with the results in the hemolysis experiment. And found to be characterized by multiple ABC transporter protein genes, all of which behaved innocuously, and that these ABC transporter proteins were associated with the formation of podoplanar polysaccharides or hydrolases. Such as the bile salt hydrolase-related transporter that transports conjugated bile acids to the intestines and reduces intestinal reabsorption of bile acids, which in turn forces the host liver to utilize more cholesterol to synthesize new bile acids and reduces the serum cholesterol level[36]. Additionally, several lipid transporter genes were detected in *L. rhamnosus* GYX-9, which are responsible for transporting phospholipids as well as glucosylceramides and glycosphingolipids[37]. Furthermore, there were 210 resistance-related genes, and *L. rhamnosus* GYX-9 had a total of 35 antibiotic-related genes for macrolide antibiotics, 16 fluoroquinolone antibiotics, and 15 aminoglycoside antibiotics (Fig.4B), which is basically in line with the results of the previous *L. rhamnosus* GYX-9 resistance test.

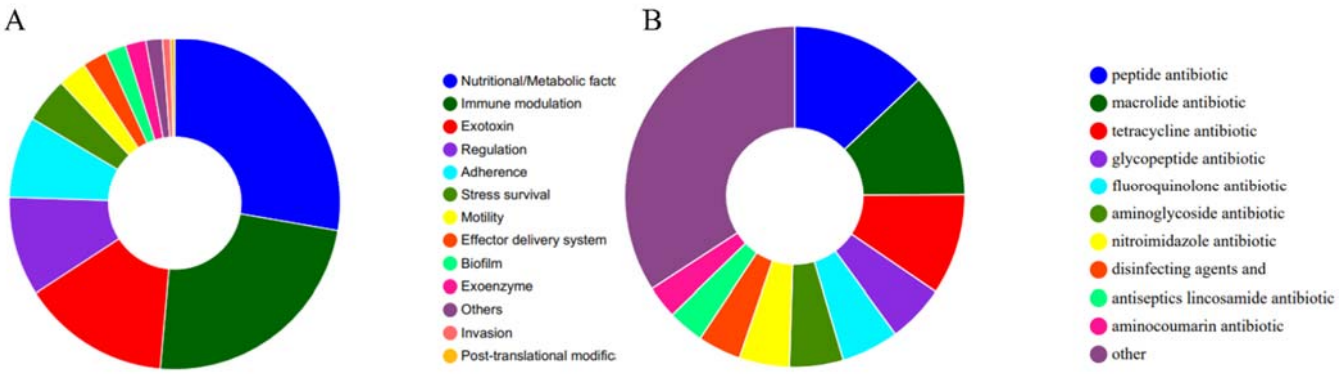

Fig.4 Pathogenic system analysis (A) Virulent factor (VFDB) stastistic, (B) Antibiotic resistance gene prediction
Note: The first and fourth circles of the circle diagram from the outside to the inside are the CDS on the positive and negative strands, and different colors indicate different COG functional classifications; the second and third circles are the CDS, tRNA, and rRNA on the positive and negative strands, respectively; the fifth circle is the GC content; and the sixth circle is the GC-Skew value, and the specific algorithm is G-C/G+C.

3.5 Functional metabolite analysis based on whole-genome information

L. rhamnosus GYX-9 exhibits strong α-amylase inhibitory and cholesterol-lowering capabilities *in vitro*. Combining this with the lipid transport genes identified in its genome, we further analyzed its metabolic network through KEGG pathway annotation. A network of molecular interactions and reactions within the species was obtained through KEGG pathway annotation to elucidate its underlying metabolic pathways. Comparing the KEGG database, a total of 1,547 functional genes were annotated in the *L. rhamnosus* GYX-9 genome, which were categorized into six major groups: cellular processes, environmental information processing, genetic information processing, human diseases, metabolism, and organismal systems. The largest number of these are functional genes related to metabolism (Fig.5). Carbohydrate metabolism encompasses processes such as gluconeogenesis/glycolysis and the TCA cycle (Tables S5 and S6). In the lipid degradation pathway, including acetaldehyde dehydrogenase/alcohol dehydrogenase [EC: 1.2.1.10 1.1.1.1], aryl alcohol dehydrogenase [EC: 1.1.1.90], and acetyl-CoA-acetyltransferase [EC: 2.3.1.9] are significantly enriched in the *L. rhamnosus* genome. Lipid oxidation produces many harmful aldehydes[38], and acetaldehyde dehydrogenase can use a variety of aldehydes as substrates and convert them into carboxylic acids that can be metabolized and utilized by the human body, which in turn serves to eliminate the harmful oxidation products[39]. Acetyl-CoA acetyltransferase participates in the synthesis and catabolism of acetyl-CoA, primarily functioning as a transfer enzyme, but also involved in fatty acid metabolism and lipid metabolism[40]. Research has reported up-regulation of ACAT2 expression to enhance the regulatory ability of bovine hepatocytes (BHEC) to maintain lipid homeostasis ameliorates BHBA-induced lipid metabolism disorders[41]. In particular, it has been found that acetaldehyde dehydrogenase 2 (ALDH2) affects cholesterol metabolism by regulating the protein stability of a key rate-determining enzyme, 3-Hydroxy-3-methylglutaroyl-CoA reductase (HMGCR), during hepatic cholesterol synthesis from scratch[42].

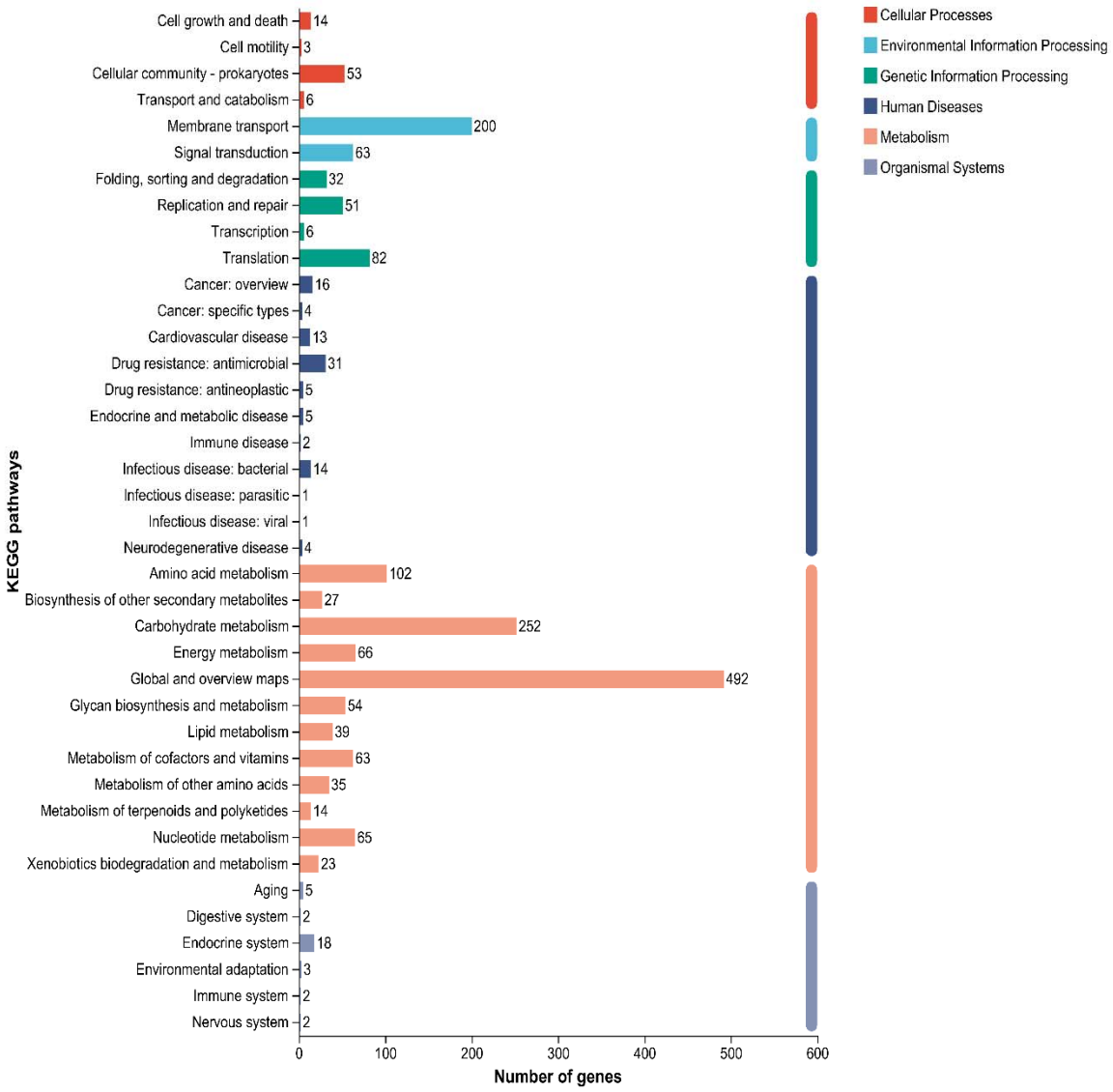

Fig.5 KEGG gene functional annotation

A total of 2,125 genes were annotated, with a notable predominance of biomolecule function-related genes (Fig.6). Among the bioprocess-related genes, phosphorylation (GO: 0016310, 88), protein hydrolysis (GO: 0006508, 58), and carbohydrate metabolism (GO: 0005975, 50) were particularly predominant. Within the carbohydrate metabolism-related genes, those encoding L-ribulose-5-phosphate 3-epimerase, β-galactosidase, and FGGY family carbohydrate kinase were included. These enzymes play direct or indirect roles in processes such as carbohydrate metabolism and oxidative stress. For instance, β-galactosidase may alleviate hyperlipidemia by producing oligosaccharides and other substances that alter the host's intestinal flora[43].

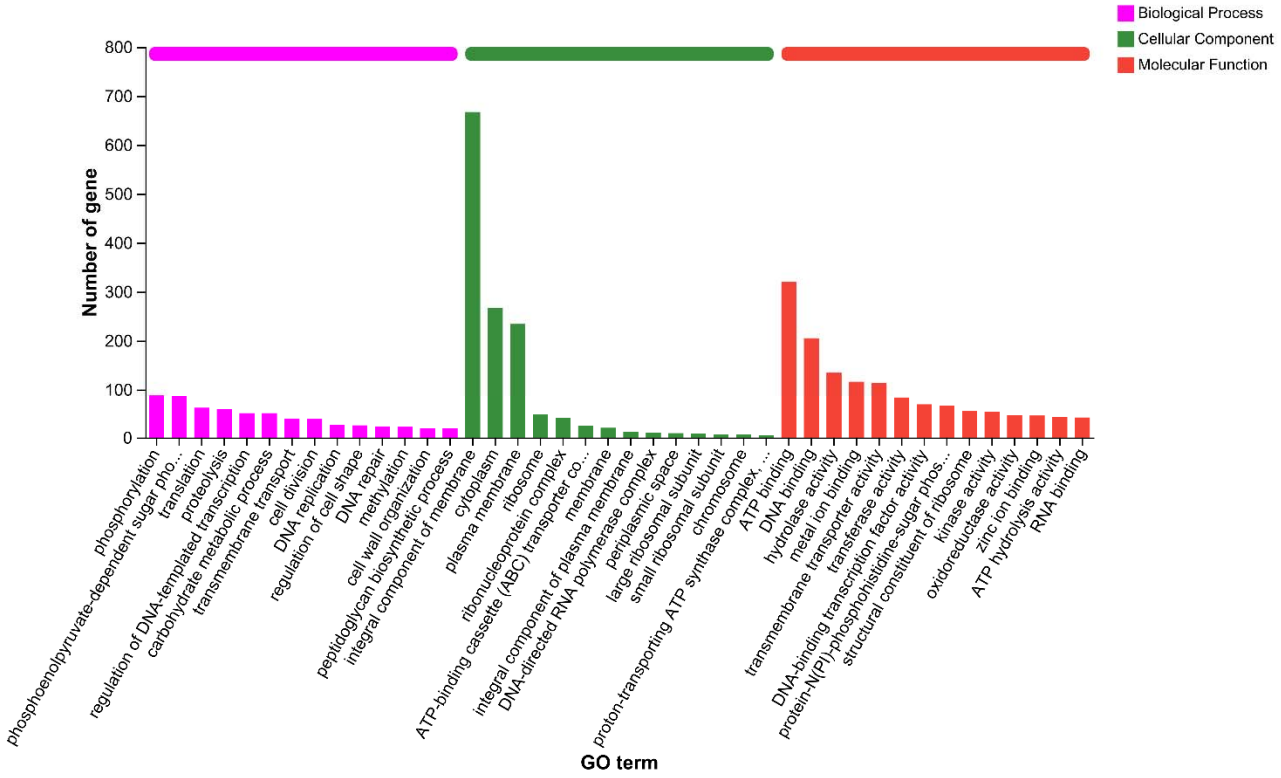

Fig.6 GO function annotation

3.6 Carbohydrate active enzyme (CAZy) analysis

Carbohydrate-active enzymes are responsible for the biosynthesis and breakdown of carbohydrates and sugar-fixings. They are involved in many metabolic pathways and are important for health. *L. rhamnosus* GYX-9 included a total of 87 CAZy enzyme genes, including 4.59% auxiliary activities (AA), 17.24% carbohydrate esterases (CE), 45.97% glycoside hydrolases (GH), and 32.18% glycosyl transferases (GT). The two fractions, GHs and GTs, together accounted for 78.16% of all the carbohydrate enzyme-related genes in *L. rhamnosus* GYX-9 (Fig.7). It has been demonstrated that GHs can hydrolyze or rearrange glycosidic bonds, whereas GTs are involved in the biosynthesis of disaccharides, oligosaccharides, and polysaccharides by catalyzing the formation of glycosidic bonds between them, and GHs have a great potential to hydrolyze complex carbohydrates, and they are considered to be key enzymes involved in carbohydrate metabolism[44]. GHs are capable of degrading the most abundant biomasses such as starch, cellulose and hemicellulose[18]. In the family of GHs, which mainly consists of six GH1s and eleven GH13s, which allow *L. rhamnosus* GYX-9 to efficiently metabolize carbohydrates, producing glycosides and saponins that act as podoplanar polysaccharide precursors, conferring resistance to undesirable environments. Among them, *L. rhamnosus* GYX-9 contains 6-phospho-β-glucosidase [EC: 3.2.1.86], 6-phospho-β-galactosidase [EC: 3.2.1.85], α-phosphotrehalase [EC: 3.2.1.93], glycoside hydrolase family 13 protein [EC: 3.2.1.54 3.2.1.133 3.2.1.135] etc., which are not directly involved in lipid metabolism processes but may regulate glucose-lipid metabolism by modulating the intestinal flora through the production of prebiotics or by influencing blood glucose levels through participation in glycogen synthesis and catabolism processes. *L. rhamnosus* contains four AAs genes,

of which the AA1 enzyme, a polymetallic oxidase that uses oxygen as a receptor, protects cells from oxidative damage and provides some antioxidant effects[45].

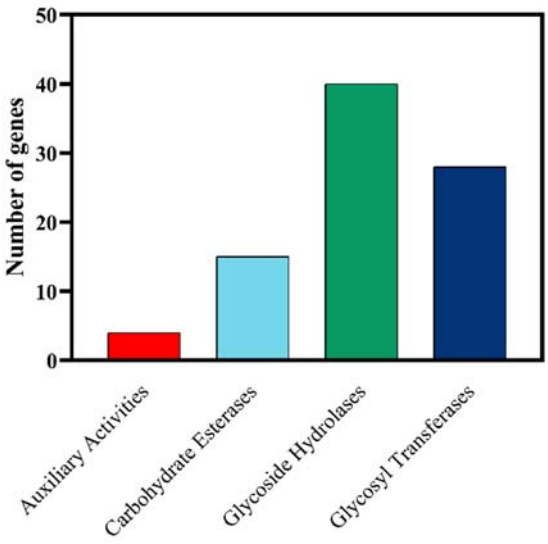

Fig.7 carbohydrate active enzyme

3.7 Genomic information mining and prediction

Three cold shock protein (*cspA*), four heat shock proteins and four alkaline shock protein (*asp23*)-related genes were found in the whole genome of *L. rhamnosus* GYX-9. Conditions such as low temperature induce the expression of the cold shock protein gene (*cspA*), which binds to single-stranded DNA and shortens the cold shock time due to the rapid decrease in temperature, allowing microorganisms to acclimatize to low temperatures more quickly while promoting protein synthesis. Heat shock proteins are proteins that are induced after stimulation by heat and other factors, and they are a class of proteins that can regulate the stress response and protect the organism against cellular damage, and they play an important role in the stress response of the organism. *asp23* family members are commonly found in Gram-positive bacteria, and the protein was found to be induced after alkaline shock[46]. It has been shown that deletion or down-regulation of *asp23* leads to cell wall thinning and enhanced cellular autolysis[47]. Among the secreted proteins of GYX-9, we identified genes associated with the synthesis of surface proteins, including the LPXTG cell wall anchoring structural domain-containing protein (GO: 0016021) and the SLPA structural domain *(cwlO*, GO: 0016787), enolase (*eno*, [EC: 4.2.1.11]), and also a gene encoding the mucus adhesion promoting protein mapA gene that encodes the mucus adhesion-promoting protein mapA (Table S7). This provides a basis for the ability of GYX-9 to adhere to mucin and collagen, suggesting that it has the potential to adhere to the gut for probiotic effects. In addition, the genome of *L. rhamnosus* GYX-9 also contains genes related to acid and bile tolerance, immune regulation, antibacterial activity, and lipid metabolism (Table S8).

3.8 In vivo lipid-lowering activity of L. rhamnosus GYX-9

3.8.1 Changes in mouse weight

Changes in body weight during the feeding period for each group of mice are shown in Table S9. Compared to the Control group, mice in the Model group exhibited a 15-20% increase in body weight,

confirming the successful establishment of the obesity model. During the 6-week gavage intervention period, the Control group gained 3.18 g, while the Model group gained 3.03 g. Weight loss became more pronounced in the sixth week of intervention. The weight gain in the HFD + *L. rhamnosus* GYX-9 group and the drug-positive Control group was 3.23 ± 2.32 g and 2.02 ± 1.42 g, respectively, with no statistically significant difference observed (Fig.8A).

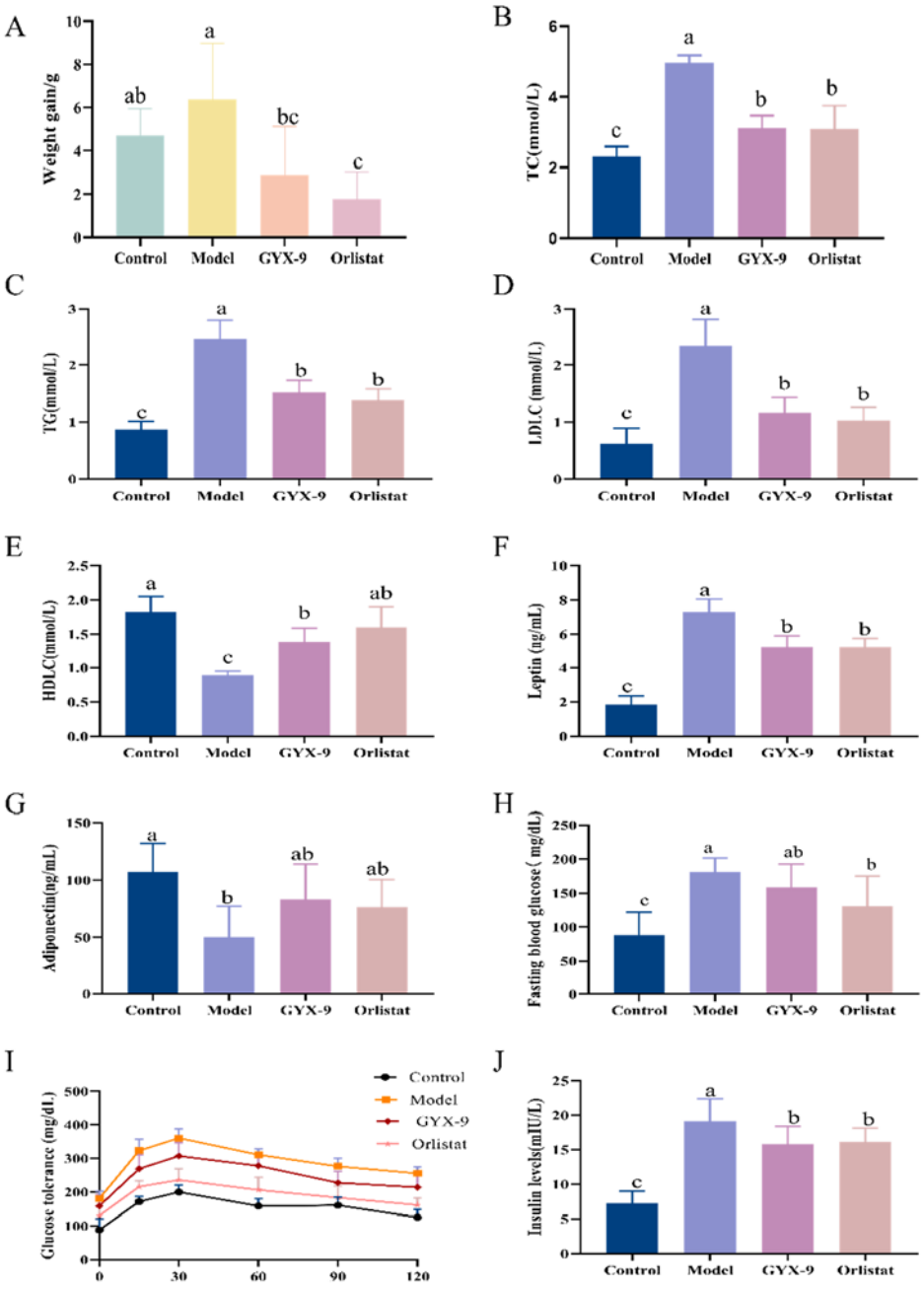

Fig.8 Effect of *L. rhamnosus* on (A) Weight gain; (B) TC; (C) TG; (D) LDLC; (E) HDLC; (F) Leptin; (G) Adiponectin; (H) Fasting blood glucose; (I) Glucose tolerance and (J) Insulin levels in high-fat mice. Data are presented as mean ± SEM. Significant differences ($P < 0.05$) among groups were analyzed by one-way ANOVA, followed by Duncan's multiple comparison test to identify specific group differences.

3.8.2 L. rhamnosus GYX-9 improves lipid metabolism disorders

After continuous high-fat feed feeding, mice in the model group exhibited abnormal disorders of lipid metabolism. Compared with the Model group, both the *L. rhamnosus* GYX-9 group and the positive Control

group significantly reduced the serum levels of TC, TG, and LDL-C. In particular, *L. rhamnosus* GYX-9 decreased TG levels to (1.52 ± 0.20) mmol/L and increased HDL-C levels by 155.02% ($P < 0.05$), close to the levels observed in the Control ($P < 0.05$) (Fig.8B-E). The results indicated that *L. rhamnosus* GYX-9 could improve lipid metabolism disorders induced by high-fat diet in mice by lowering the serum levels of TC, TG, and LDL-C, and elevating the HDL-C content.

HFDs significantly increased serum leptin levels and decreased adiponectin content (Fig.8F-G), compared with the Model group, the serum leptin level of mice in *L. rhamnosus* GYX-9 group decreased 71.23%, and the lipocalin content increased 166.41% ($P < 0.05$), *L. rhamnosus* GYX-9 can more effectively improve the leptin resistance and decrease the lipocalin content of mice due to obesity, and it has important significance for the prevention of obesity in mice.

3.8.3 L. rhamnosus GYX-9 improves glucose metabolism disorders

The fasting blood glucose in the GYX9 group was not significantly different from that of the Model group, but there was a certain downward trend. The blood glucose levels of each treatment group were significantly lower than those in the Model group at the 2-hour time point. The blood glucose trend in the GYX-9 group was significantly more stable and more towards normal levels. The level of serum insulin in mice in the GYX-9 group was significantly decreased by 17.65% (Fig.8H-J), indicating that gavage of *L. rhamnosus* GYX-9 to mice had a better tolerance to glucose injections, and it had a protective effect against high-fat diet-induced hyperinsulinemia in mice, which is in agreement with the experimental results of Han et al[48].

3.8.4 L. rhamnosus GYX-9 attenuates hepatic fat accumulation and oxidative stress in high-fat mice

The level of FFA in the liver is an important indicator for evaluating the degree of lipid accumulation in the liver of mice. Compared with the Control group, the liver coefficient and epididymal fat coefficient of mice in the model group increased significantly ($P < 0.05$) (Fig.9A-C), indicating that the HFD could lead to the abnormal liver status and large accumulation of fat in mice. The liver coefficient and epididymal fat coefficient of the GYX-9 group decreased by 15.33% and 22.61%, respectively, compared with the Model, which significantly reduced the hepatic FFA level caused by the HFD, ($P < 0.05$), indicating that *L. rhamnosus* GYX-9 could significantly inhibit high-fat diet-induced fat accumulation in mice.

CAT and SOD are important antioxidant enzymes in the body, indirectly reflecting liver injury. Although *L. rhamnosus* GYX-9 intervention enhanced hepatic SOD activity, the increase was not statistically significant, and levels did not return to those of the control group. After the intervention of the GYX-9 group and the positive control group, the content of MDA in the liver cells was reduced, although there was no significant difference, and the level of intracellular lipid peroxidation was decreased (Fig.9D-F). CAT activity in the liver of the high-fat model group was significantly reduced, and CAT activity in the liver of the GYX-9 group was significantly elevated by 35.5% compared with that of the high-fat group ($P < 0.05$).

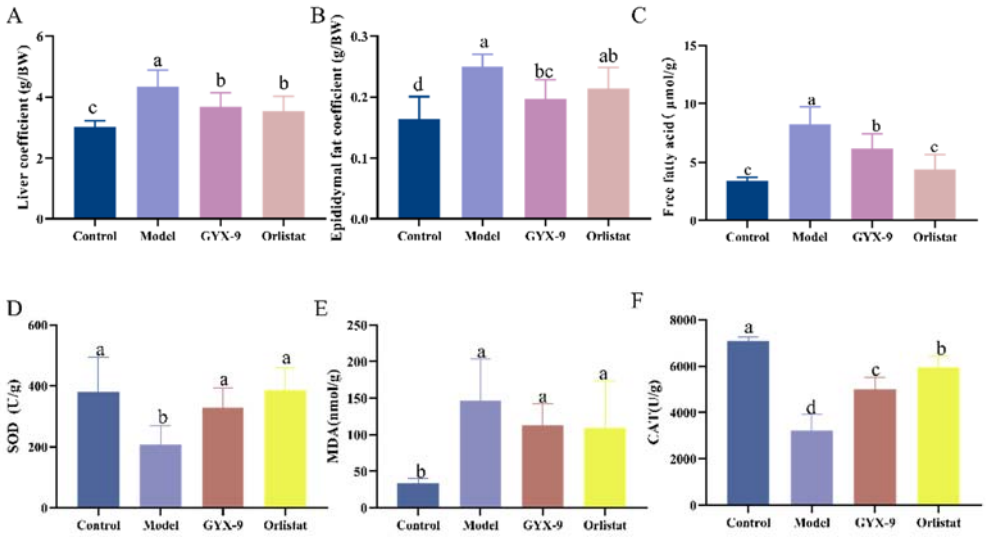

Fig.9 Effects of *L. rhamnosus* on (A) liver coefficient; (B) epididymal fat coefficient in high-fat mice (C) free fatty acid; (D)SOD; (E) MDA; (F) CAT. Data are presented as mean ± SEM. Significant differences ($P < 0.05$) among groups were analyzed by one-way ANOVA, followed by Duncan's multiple comparison test to identify specific group differences.

3.9 L. rhamnosus GYX-9 regulates colon immunity

Lipid metabolism disorders can induce inflammatory responses through multiple pathways. The Model group exhibited pronounced colonic tissue inflammation, characterized by a marked elevation in pro-inflammatory cytokines, including TNF-α, IL-1β, and IL-6, alongside a significant reduction in the anti-inflammatory cytokine IL-10 ($P < 0.05$) (Fig.10). Compared with the Model group, the GYX-9 group significantly decreased the levels of TNF-α, IL-1β, and IL-6, decreased by 32.63%, 52.65%, and 29.15%, respectively, and significantly increased IL-10 levels to (170.55 ± 36.34) pg/mL($P < 0.05$). The elevated levels of inflammatory factors were alleviated, which in turn alleviated the body inflammation guided by the HFD.

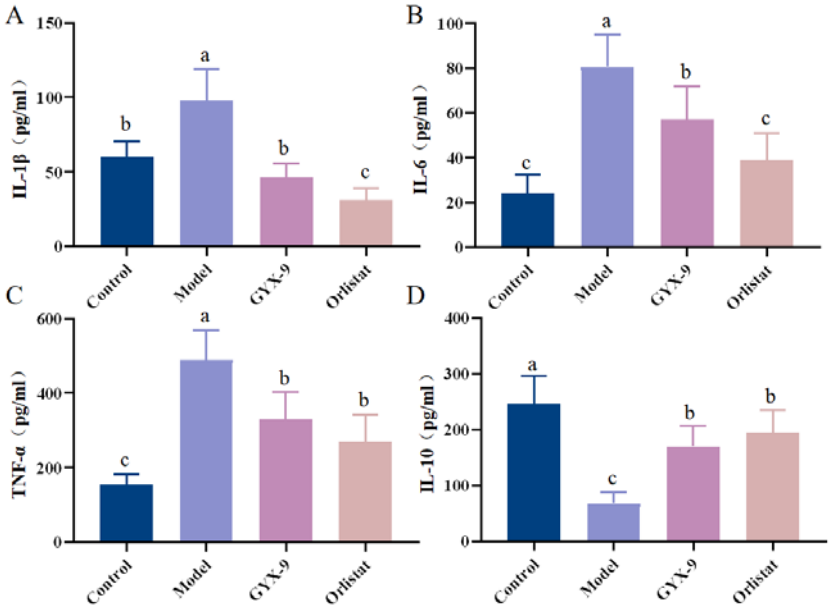

Fig.10 Effect of *L. rhamnosus* on inflammatory factors in colon tissue of high-fat mice (A) IL-1β; (B) IL-6; (C) TNF-α; (D) IL-10. Data are presented as mean ± SEM. Significant differences ($P < 0.05$) among groups

were analyzed by one-way ANOVA, followed by Duncan's multiple comparison test to identify specific group differences.

3.10 L. rhamnosus GYX-9 improves intestinal microbial community structure and dysbiosis

Obesity and gut flora are intricately linked. On the one hand, obesity can lead to an imbalance in gut flora, and on the other hand, this imbalance can exacerbate obesity. Venn diagrams illustrated the shared and unique operational taxonomic units (OTUs) among the different groups. The GYX-9 group exhibited the most number of endemic OUTs, indicating that *L. rhamnosus* GYX-9 had an effect on the diversity of the intestinal flora (Fig.11A). Compared with the Control group, Simpson's index decreased and Shannon's index increased significantly ($P < 0.05$) in the GYX-9 group, indicating that the *L. rhamnosus* GYX-9 was able to enhance the diversity of intestinal flora in high-fat mice. In addition, the coverage values of all groups were higher than 0.995, indicating a high coverage of the samples (Fig.11B-D).

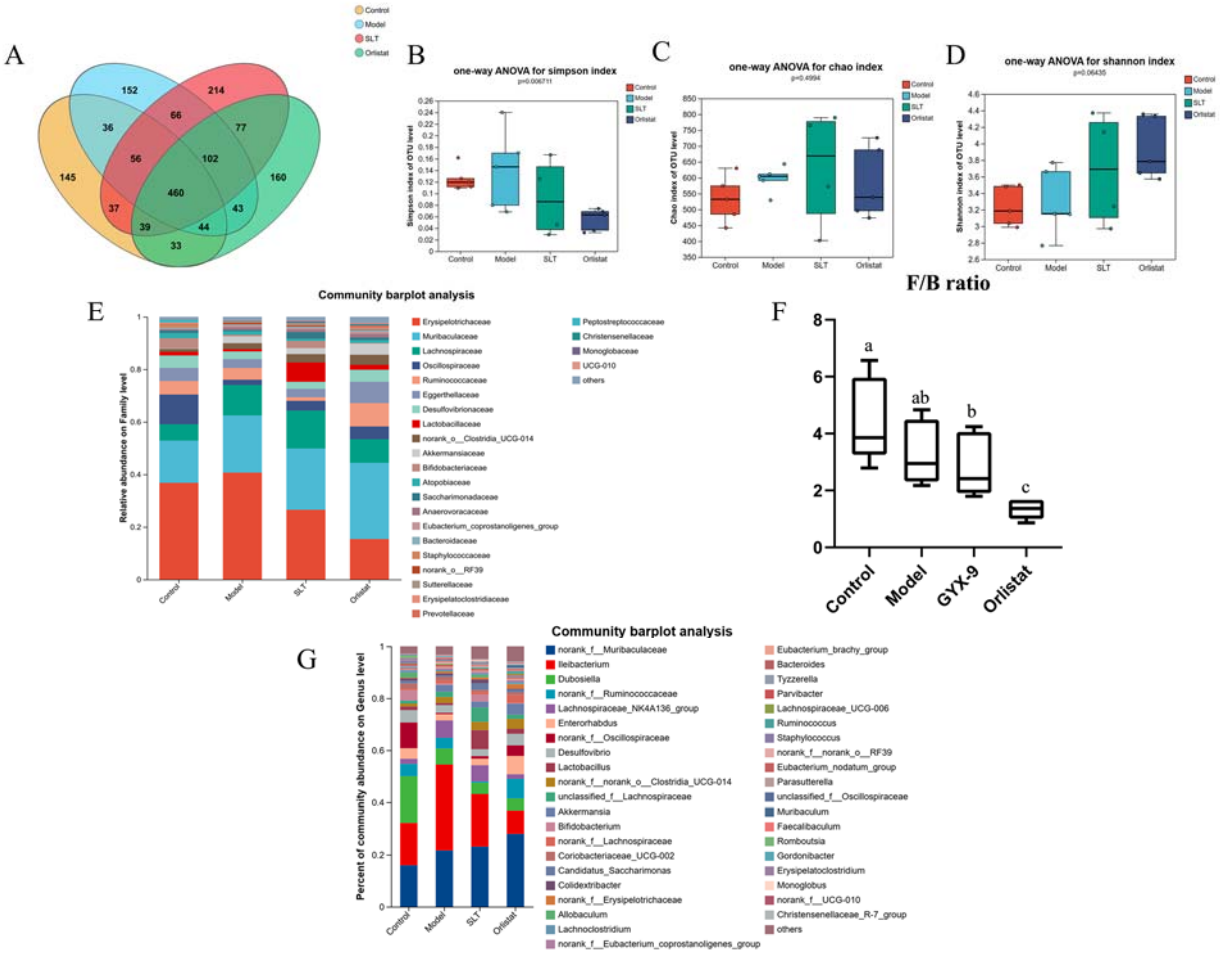

Fig.11 Effects of *L. rhamnosus* GYX-9 on gut microbiota diversity and composition. (A) Venn diagram; (B) Simpon index; (C) Chao1; (D) Shannon index; (E) Relative abundance of gut microbiota at the phylum level; (F) *Firmicutes/Bacteroidetes* ratio; (G) Relative abundance of gut microbiota at the genus level. Data are presented as mean ± SEM. Significant differences ($P < 0.05$) among groups were analyzed by one-way ANOVA, followed by Duncan's multiple comparison test to identify specific group differences.

Firmicutes, *Bacteroidetes* (F/B) has been shown to increase in obese animals and obese humans. Compared with Control and Model groups, F/B was significantly reduced in GYX-9 group and Orlistat

group (Fig.11F), indicating that *L. rhamnosus* GYX-9 can prevent and improve obesity by decreasing the ratio of *Firmicutes* to *Bacteroidetes* and thus may play a role in the prevention and amelioration of obesity.

At the genus level, the intestinal flora mainly included beneficial bacteria such as *norank_f_Muribaculaceae, Dubosiella, Lachnospiraceae_NK4A136_group, Lactobacillus, Enterorhabdus, Bifidobacterium; Ileibacterium, Desulfovibrio, norank_f_Oscillospiraceae* and other harmful bacteria. The relative abundance of beneficial bacteria such as *Bifidobacterium* and *Colidextribacter* was significantly reduced in the Model compared to the Control ($P < 0.05$). The relative abundance of *Bifidobacterium, Candidatus_Saccharimonas, Romboutsia, Erysipelatoclostridium, Colidextribacter* and other body weight related bacteria was significantly increased ($P < 0.05$) in the GYX-9 group compared to the Model group. The relative abundance of the genus level of the flora thereby achieving the alleviation of obesity in high-fat mice (Fig.12).

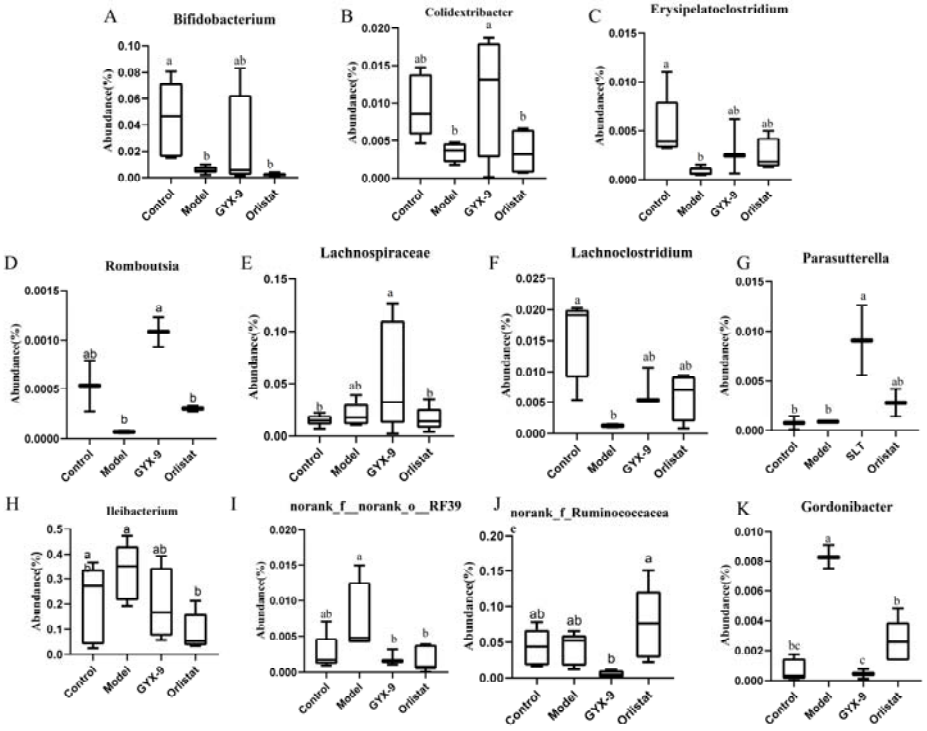

Fig.12 Changes in the genera of intestinal microbial fractions in mice after intervention with *L.ramnosus* GYX-9. (A) *Bididobacterium* abundance; (B) *Colidextribacter* abundance; (C) *Erysipelatoclostridium* abundance; (D) *Romboutsia* abundance; (E) *Lachnospiraceae* abundance; (F) *Lachnoclostridium* abundance; (G) *parasutterella* abundance; (H) *Ileibacterium* abundance; (I) *norank_f_norank_o_RF39* abundance; (J) *norank_f_Ruminococcacea* abundance; (K) *Gordonibacter* abundance. Data are presented as mean ± SEM. Significant differences ($P < 0.05$) among groups were analyzed by one-way ANOVA, followed by Duncan's multiple comparison test to identify specific group differences.

LEfSe analysis was utilized to highlight the differential representation of microbial species between the different groups (Fig.S1). The HFD partially disturbed the balance of the gut flora. Notably, an increase in beneficial bacterial enrichment was observed in the treatment group. Specifically, the enrichment of *Colidextribacter* and *Parasutterella* in the GYX-9 group contributed to an increase in the abundance of beneficial bacteria, favoring the reduction of obesity.

3.11 Correlation analysis between gut microbial communities and obesity-related biochemical indicators

By analyzing the correlation between gut microbes and biochemical indicators, etc., through Spearman correlation coefficient, combined with the main enriched genera and the gut microbes significantly regulated by the *L. rhamnosus* GYX-9, we found that the relative abundance of *Ileibacterium* showed a positive correlation with the pro-inflammatory factors IL-1β, IL-6, AST, and leptin; *norank_f_norank_o_RF39* Relative abundance was positively correlated with IL-1β and showed deleterious effects; *Erysipelatoclostidium* and *Lachnoclostidium* relative abundance was negatively correlated with IL-6, TNF-α, LPS, TG, and LDLC, and positively correlated with HDLC, lipocalin, and CAT; *Romboutsia* relative abundance was positively correlated with TNF-α, fasting blood glucose were negatively correlated. The relative abundance of *Romboutsia* was negatively correlated with TNF-α and fasting blood glucose. *L. rhamnosus* GYX-9 alleviated obesity, colonic inflammation by down-regulating *Ileibacterium, norank_f_norank_o_RF39*, and up-regulating *Erysipelatoclostidium, Lachnoclostidium, Romboutsia* (Fig.13).

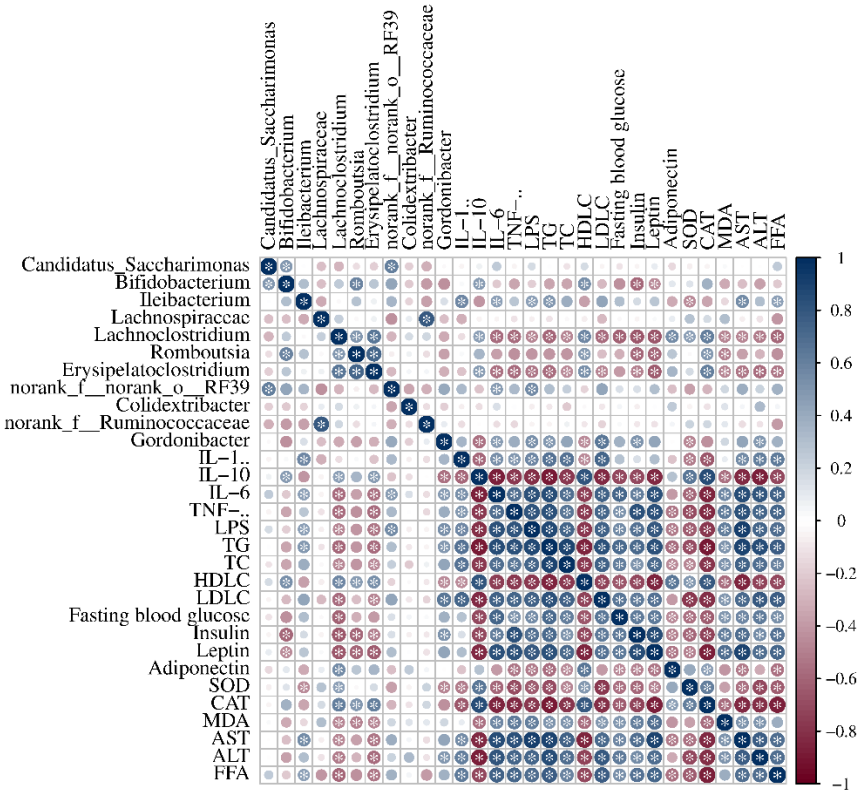

Fig.13 Spearman correlation between obesity-related biochemical indexes and intestinal microbial communities at the genus level.*$P < 0.05$.

4. Discussion

Probiotics have been proven to be safe, and many LAB have been shown to regulate lipid metabolism and alleviate obesity. The mechanisms by which various LAB regulate lipid metabolism differ, including their effects on lipid assimilation and adsorption[49], regulation of lipid metabolism-related transcription factors (such as short-chain fatty acids, conjugated linoleic acid, and ferulic acid esterase), influence on lipid transport and absorption[50, 51]. Ultimately, these regulatory mechanisms are determined by the genetic makeup of LAB. Sun et al[52] conducted whole-genome sequencing of selected *Lactobacillus plantarum* and found that

the presence of genes encoding antioxidant enzymes, antimicrobial peptides, bacteriocins, stress response proteins, and cholesterol-lowering factors (such as genes related to ABC transporters for sulfated lipids) is closely associated with the functional phenotypes of different strains. This highlights the importance of genomic analysis in predicting and understanding the probiotic potential of LAB, which provides a theoretical basis for our study focusing on the genomic characteristics and functional verification of *L. rhamnosus* GYX-9.

Currently, there are few studies on the whole-genome characteristics of lipid-lowering probiotics. Compared with *Lactobacillus plantarum* HOM221715[53], which has been reported to have lipid-lowering effects, *L. rhamnosus* GYX-9 shares certain similarities in terms of immune regulation, antibacterial activity, and acid and bile salt tolerance. However, *L. rhamnosus* GYX-9 contains more lipid metabolism genes, including six *tagE*, three *glpQ*, and three *fabG* genes, whereas *Lactobacillus plantarum* HOM2217 possesses only one copy of each of these genes. However, compared to *Lactobacillus acidophilus* AM13-1[54], *L. rhamnosus* GYX-9 lacks the *cbh* gene. This indicates that *L. rhamnosus* GYX-9 does not achieve its cholesterol-lowering effect by promoting the coprecipitation of bile acids and cholesterol. *L. rhamnosus* GYX-9 may improve lipid metabolism disorders through genes such as *pckA* and *pyc*, which are involved in the TCA cycle. Liu's[55] research findings indicate that a high-fat diet reduces TCA metabolism by 37.48%, and metformin achieves its lipid-lowering effect by enhancing TCA metabolism. The TCA cycle is one of the key steps in fatty acid oxidation, helping to reduce fat levels in the body. Fatty acids are broken down into acetyl-CoA through β-oxidation, and acetyl-CoA enters the TCA cycle for further oxidation and energy release. Additionally, phosphoenolpyruvate carboxykinase (PEPCK) is a rate-limiting enzyme in hepatic gluconeogenesis, which helps maintain stable blood glucose level, as evidenced by glucose tolerance in mice[56]. The genome is also significantly enriched in aldehyde dehydrogenase [EC: 1.2.1.10 1.1.1.1]. According to Zhong's[42] research, aldehyde dehydrogenase 2 (ALDH2) influences cholesterol metabolism by regulating the protein stability of HMGCR, a key rate-limiting enzyme in hepatic cholesterol de novo synthesis. We speculate that the lipid-lowering mechanism of *L. rhamnosus* GYX-9 may also involve this pathway.

Long-term dysregulation of lipid metabolism leads to excessive accumulation of lipids in the liver, inducing a lipotoxic state, triggering oxidative pathways in the body, producing large amounts of reactive oxygen species, and causing oxidative stress. Excessive oxidative stress is closely related to the pathogenesis of obesity-related syndromes. Additionally, genes encoding L-ribulose-5-phosphate 3-epimerase (GO: 0044723; GO: 0044261), provides NADPH to cells, which is crucial for glutathione regeneration. Glutathione can detoxify H_2O_2, thereby protecting cells from oxidative stress damage[57].

The gut microbiota plays a pivotal role in the development of obesity, and its imbalance can both result from and exacerbate obesity. Our study found that *L. rhamnosus* GYX-9 intervention significantly reshapes the gut microbiota structure of HFD-fed mice, which is closely related to its genomic features. The genome of *L. rhamnosus* GYX-9 contains genes associated with acetate/propionate synthesis pathways, including *ackA*,

scpA, and *pta*. Short-chain fatty acids (SCFAs) such as acetate and propionate are key metabolic products of gut microbiota. Propionate can interact with adipose tissue to increase mRNA expression and leptin secretion[58], while both acetate and propionate can promote the secretion of antimicrobial peptides by interacting with intestinal epithelial cells and the FFAR2 receptor[59]. These SCFAs, combined with the antimicrobial genes of *L. rhamnosus* GYX-9, contribute to reducing the abundance of harmful bacteria in the gut. Consistent with this, our results showed that *L. rhamnosus* GYX-9 intervention increased the diversity of the gut microbiota, downregulated the relative abundance of harmful genera including *Ileibacterium* and *Desulfovibrio*.

Enterobacteriaceae in the gut have been shown to correlate positively with serum lipopolysaccharide levels, while *Bifidobacteria* correlate positively with IL-10 and high-density lipoprotein cholesterol. Consistent with Liu's findings, *Romboutsia* correlate negatively with body weight, fasting blood glucose, and insulin levels[60]. This series of correlations indicate that *L. rhamnosus* GYX-9 alleviates obesity and colonic inflammation by regulating the abundance of specific gut microbiota genera. Consistent with previous studies, *L. rhamnosus* TR08 improves dyslipidemia by increasing *Bifidobacterium* abundance[61], and *Romboutsia* sedimentorum can utilize glucose to produce acetic acid and isobutyric acid, which is beneficial for reducing obesity[62]. Additionally, Huang et al[63]. found that the expression levels of cadherin-11, IL-17, and TLR2 are negatively correlated with *Candidatus_Saccharimonas*, and the absence of TLR2 can eliminate diabetic and obese phenotypes—providing further support for the role of microbiota modulation in *L. rhamnosus* GYX-9's anti-obesity effects.

The ability of probiotics to adhere to the intestinal mucosa is a prerequisite for their functional activity, and surface proteins play a significant role in this adhesion process. Additionally, surface proteins possess certain physiological functions and may also be indirectly associated with lipid-lowering pathways. Our results indicate that the genes encoding secreted proteins in *L. rhamnosus* GYX-9 contain the LPXTG cell wall-anchored domain-containing protein (GO: 0016021), the surface layer protein A domain (*cwlO*, GO: 0016787), enolase (*eno*, [EC: 4.2.1.11]), and the mucus adhesion-promoting protein mapA. Surface proteins is a unique natural coat of Lactobacillus species, which not only helps them resist external threats but also serves as an adhesion tool to promote their colonization in the intestine. Currently, only LPxTG has been shown to participate in the adhesion between Lactobacillus species and intestinal cells[64]. Additionally, mapA-mediated adhesion may facilitate adhesion to Caco-2 cells[65]. Therefore, the high adhesion rates to mucin and collagen suggest that *L. rhamnosus* can stably colonize the intestine, providing conditions for exerting functional characteristics and regulating intestinal microbiota balance. Based on SDS-PAGE results, the potential surface protein components enolase and SpaC of *L. rhamnosus* GYX-9 were found to not only possess anti-adhesive properties but also protect cells from the toxic effects of Staphylococcus aureus[66]. Furthermore, our previous studies have shown that the S-layer protein derived from Lactobacillus acidophilus CICC6074 exhibits intestinal immune regulatory activity, which may help alleviate ulcerative colitis[67]. Additionally, the surface protein of *Lactobacillus paracasei* K56 has been reported to possess lipid-lowering

activity[68]. Whether the surface proteins of *L. rhamnosus* GYX-9 possess similar functional properties warrants further investigation.

In summary, *L. rhamnosus* GYX-9 exerts anti-obesity effects through a multi-pathway driven by its unique genomic characteristics: (1) Genes involved in the TCA cycle (*pckA, pyc,* etc.) and aldehyde dehydrogenase regulate lipid and cholesterol metabolism; (2) Genes encoding L-ribulose-5-phosphate 3-epimerase alleviate hepatic oxidative stress; (3) Genes related to acetate/propionate synthesis (*ackA, scpA, pta*) promote SCFAs production, reshaping the gut microbiota structure and reducing harmful bacteria abundance; (4) Surface protein synthesis genes (*eno, cwlO, mapA*) enhance intestinal adhesion, facilitating stable colonization and functional exertion; (5) Immune regulation-related genes (*dlt, agr,* etc.) modulate colonic inflammation by reducing pro-inflammatory factors and increasing anti-inflammatory cytokines. Regulating the gut microbiota may be a key target in these pathways, indirectly influencing lipid metabolism and immune responses by stabilizing the intestinal flora. First, intestinal adhesion forms the foundation for the lipid-lowering effects of *L. rhamnosus* GYX-9. The strain modulates the gut microbiota through its strong adhesion properties and its ability to produce short-chain fatty acids. These microbiota changes further enhance lipid metabolism and antioxidant activity. Additionally, the genes involved in lipid metabolism, antioxidant defense, and immune regulation work together in an interconnected network, collectively driving the lipid-lowering effects of *L. rhamnosus* GYX-9. While this study demonstrates the anti-obesity potential of *L. rhamnosus* GYX-9, the molecular mechanisms mediated by key genes in lipid metabolism and energy homeostasis remain unclear. Future work should employ multi-omics approaches to elucidate the regulatory networks governed by GYX-9 in host tissues.

5. Conclusion

Our data indicate that the *L. rhamnosus* GYX-9 genome possesses genes such as *dlt* and *agr* associated with immune regulation. Mice in the treatment group exhibited significantly reduced colonic IL-1β levels and elevated IL-10 levels. It also possesses genes involved in the tricarboxylic acid cycle, such as *pckA* and *pyc*, and can synthesize enzymes like aldehyde dehydrogenase and PEPCK. Treated mice exhibited reduced hepatic fat content and regulated lipid metabolism. The alleviation of hepatic oxidative stress in high-fat mice may be associated with L-ribulose-5-phosphate 3-epimerase. Contains genes associated with acetate/propionate synthesis pathways, such as *ackA, scpA*, and *pta*. Treated mice exhibited increased gut microbial diversity, with elevated beneficial bacteria and reduced harmful bacteria. Additionally, it contains genes related to surface protein synthesis *(eno, cwlO, mapA*) that protect bacterial cells and enhance intestinal adhesion. Evidence demonstrates that *L. rhamnosus* GYX-9 modulates lipid metabolism, reduces hepatic fat accumulation, alleviates hepatic oxidative stress, regulates gut microbiota, and corrects colonic immune dysregulation, ultimately leading to weight reduction.

Declaration of competing interest

The authors declare that they have no known competing financial interests or personal relationships that could have appeared to influence the work reported in this paper.

Appendix A. Supplementary data

The last is the Supplementary data to this article.

Data availability

Data will be made available on request.

Reference

1.Ng M, Gakidou E, Lo J, et al, Global, regional, and national prevalence of adult overweight and obesity, 1990–2021, with forecasts to 2050: a forecasting study for the Global Burden of Disease Study 2021, *The Lancet*, 405(2025) 813-838.https://doi.org/https://doi.org/10.1016/S0140-6736(25)00355-1.

2.Yang B, Wang W, Jian C, et al, Screening of the Lipid-Lowering Probiotic *Lactiplantibacillus Plantarum* SDJ09 and its Anti-Obesity Mechanism, *Appl. Biochem. Biotechnol*, 197(2025) 35-54.https://doi.org/10.1007/s12010-024-05034-x.

3.Perdomo CM, Cohen R, Sumithran P, et al, Contemporary medical, device, and surgical therapies for obesity in adults, *Lancet*, 401(2023) 1116-1130.https://doi.org/10.1016/S0140-6736(22)02403-5.

4.Wu Y, Li X, Tan F, et al, *Lactobacillus fermentum* CQPC07 attenuates obesity, inflammation and dyslipidemia by modulating the antioxidant capacity and lipid metabolism in high-fat diet induced obese mice, *J Inflamm*, 18(2021) 5.https://doi.org/10.1186/s12950-021-00272-w.

5.Ding Z, Hani A, Li W, et al, Influence of a cholesterol-lowering strain *Lactobacillus plantarum* LP3 isolated from traditional fermented yak milk on gut bacterial microbiota and metabolome of rats fed with a high-fat diet, *Food Funct.*, 11(2020) 8342-8353.https://doi.org/10.1039/D0FO01939A.

6.Wu F, Yang M, Song X, et al, Effects of viable *Lacticaseibacillus paracasei* K56 and its derived postbiotics on obesity and inflammation induced by a high-fat diet, *Food Biosci.*, 65(2025) 105999.https://doi.org/https://doi.org/10.1016/j.fbio.2025.105999.

7.Won S-M, Chen S, Lee SY, et al, *Lactobacillus sakei* ADM14 Induces Anti-Obesity Effects and Changes in Gut Microbiome in High-Fat Diet-Induced Obese Mice, *Nutrients*, 12(2020) 3703.https://doi.org/10.3390/nu12123703.

8.An HM, Kim MJ, Moon JS, et al, Antiobesity and lipid-lowering effects of *Bifidobacterium* spp. in high fat diet-induced obese rats, *Lipids Health Dis.*, 26(2012).https://doi.org/10.1186/1476-511X-10-116.

9.Li HZ, Liu F, Lu JJ, et al, Probiotic Mixture of *Lactobacillus plantarum* Strains Improves Lipid Metabolism and Gut Microbiota Structure in High Fat Diet-Fed Mice, *Front. Microbiol.*, 11(2020).https://doi.org/10.3389/fmicb.2020.00512.

10.Wu F, Ma G, Zeng Z, et al, Surface Proteins and Adhesion Properties of Lacticaseibacillus paracasei K56, *Food Science*, 45(2024) 94-102.https://doi.org/10.7506/spkx1002-6630-20240213-070.

11.Meng J, Zhang Q-X,Lu R-R, Identification and analysis of the function of surface layer proteins from three *Lactobacillus* strains, *Ann. Microbiol.*, 68(2018) 207-216.https://doi.org/10.1007/s13213-018-1335-1.

12.Aryantini NPD, Kondoh D, Nishiyama K, et al, Anchorless cell surface proteins function as laminin-binding adhesins in *Lactobacillus rhamnosus* FSMM22, *FEMS Microbiol. Lett.*, 364(2017).https://doi.org/10.1093/femsle/fnx056.

13.Dehghani S, Edalatian Dovom MR, Yavarmanesh M, et al, In vitro Evaluation of Potential Probiotic Characteristics and Survival of Human and Foodborne Lactic Acid Bacteria (*Lacticaseibacillus rhamnosus* and *Lactiplantibacillus plantarum*) in Mice Gastrointestinal Tract, *Appl. Biochem. Microbiol.*, 58(2022) S91-S101.https://doi.org/10.1134/S0003683822100052.

14.Ji Y, Park S, Park H, et al, Modulation of Active Gut Microbiota by *Lactobacillus rhamnosus* GG in a Diet Induced Obesity Murine Model, *Front. Microbiol.*, 9(2018).https://doi.org/10.3389/fmicb.2018.00710.

15.Fan SY, Chen SY,Lin L, Research progress of gut microbiota and obesity caused by high-fat diet, *Front. Cell. Infect. Microbiol.*, 13(2023).https://doi.org/10.3389/fcimb.2023.1139800.

16.Michels M, Jesus GFA, Abatti MR, et al, Effects of different probiotic strains B. lactis, *L.rhamnosus* and *L. reuteri* on brain-intestinal axis immunomodulation in an endotoxin-induced inflammation, *Mol. Neurobiol.*, 59(2022) 5168-5178.https://doi.org/10.1007/s12035-022-02906-3.

17.Kumari M, Dasriya VL, Ali SA, et al, Evaluation of antioxidant and anti-inflammatory properties of *Lacticaseibacillus rhamnosus* Ram12-derived exopolysaccharide in a D-galactose-induced liver injury mouse model, *Int. J. Biol. Macromol.*, 281(2024).https://doi.org/13624110.1016/j.ijbiomac.2024.136241.

18.Tarrah A, Pakroo S, Lemos Junior WJF, et al, Complete Genome Sequence and Carbohydrates-Active EnZymes (CAZymes) Analysis of *Lactobacillus paracasei* DTA72, a Potential Probiotic Strain with Strong Capability to Use Inulin, *Curr. Microbiol.*, 77(2020) 2867-2875.https://doi.org/10.1007/s00284-020-02089-x.

19.Liang T: The Regulatory Mechanism of Hypoglycemic and Lipid-lowering Efficacy in Probiotics Based on the Multi-omics. *Doctor thesis(in Chinese).* 2021. https://doi.org/10.27290/d.cnki.gxbqc.2021.000446.

20.Ben-Miled H, Benoit-Biancamano M-O, Ben-Mahrez K, et al, Alpha-amylase and alphaglucosidase inhibitory properties, beta-galactosidase activity, and probiotic potential of lactic acid bacteria and bifidobacteria from Apis mellifera intermissa and its products, *WORLD J MICROB BIOT*, 39(2023) 205.https://doi.org/10.1007/s11274-023-03648-7.

21.Rudel LL,Morris MD, Determination of cholesterol using o-phthalaldehyde, *J Lipid Res*, 14(1973) 364-366.https://doi.org/10.1016/S0022-2275(20)36896-6.

22.Lebeer S, Vanderleyden J,De Keersmaecker SCJ, Genes and Molecules of Lactobacilli Supporting Probiotic Action, *Microbiol Mol Biol R*, 72(2008) 728-+.https://doi.org/10.1128/Mmbr.00017-08.

23.Marbun KT, Sugata M, Purnomo JS, et al, Genomic Characterization and Safety Assessment of *Bifidobacterium breve* BS2-PB3 as Functional Food, *J Microbiol Biotechnol*, 34(2024) 871-879.https://doi.org/10.4014/jmb.2311.11031.

24.Ben-Miled H, Benoit-Biancamano MO, Ben-Mahrez K, et al, Alpha-amylase and alphaglucosidase inhibitory properties, beta-galactosidase activity, and probiotic potential of lactic acid bacteria and bifidobacteria from Apis *mellifera intermissa* and its products, *WORLD J MICROB BIOT*, 39(2023).https://doi.org/20510.1007/s11274-023-03648-7.

25.Kumari V. B. C, Huligere SS, Shbeer AM, et al, Probiotic Potential Lacticaseibacillus casei and Limosilactobacillus fermentum Strains Isolated from Dosa Batter Inhibit α-Glucosidase and α-Amylase Enzymes, *Microorganisms*, 10(2022) 1195.https://doi.org/10.3390/microorganisms10061195.

26.Romero-Luna HE, Peredo-Lovillo AG,Jiménez-Fernández M, Probiotic and Potentially Probiotic Bacteria with Hypocholesterolemic Properties, *Food Rev. Int.*, 39(2023) 689-707.https://doi.org/10.1080/87559129.2021.1926481.

27.Nami Y, Vaseghi Bakhshayesh R, Manafi M, et al, Hypocholesterolaemic activity of a novel autochthonous potential probiotic Lactobacillus plantarum YS5 isolated from yogurt, *LWT*, 111(2019) 876-882.https://doi.org/https://doi.org/10.1016/j.lwt.2019.05.057.

28.Tsai CC, Lin PP, Hsieh YM, et al, Cholesterol-lowering potentials of lactic acid bacteria based on bile-salt hydrolase activity and effect of potent strains on cholesterol metabolism in vitro and in vivo, *ScientificWorldJournal*, 2014(2014) 690752.https://doi.org/10.1155/2014/690752.

29.Brashears MM, Gilliland SE,Buck LM, Bile Salt Deconjugation and Cholesterol Removal from Media by *Lactobacillus casei*1, *J. Dairy Sci.*, 81(1998) 2103-2110.https://doi.org/https://doi.org/10.3168/jds.S0022-0302(98)75785-6.

30.Meng J, Zhang QX,Lu RR, Identification and analysis of the function of surface layer proteins from three *Lactobacillus* strains, *Ann. Microbiol.*, 68(2018) 207-216.https://doi.org/10.1007/s13213-018-1335-1.

31.Savijoki K, Nyman TA, Kainulainen V, et al, Growth Mode and Carbon Source Impact the Surfaceome Dynamics of *Lactobacillus rhamnosus* GG, *Front. Microbiol.*, 10(2019).https://doi.org/127210.3389/fmicb.2019.01272.

32.von Ossowski I, Reunanen J, Satokari R, et al, Mucosal Adhesion Properties of the Probiotic *Lactobacillus rhamnosus* GG SpaCBA and SpaFED Pilin Subunits, *Appl. Environ. Microbiol.*, 76(2010) 2049-2057.https://doi.org/10.1128/Aem.01958-09.

33.Mayo B, van Sinderen D,Ventura M, Genome analysis of food grade lactic Acid-producing bacteria: from basics to applications, *CURR GENOMICS*, 9(2008) 169-183.https://doi.org/10.2174/138920208784340731.

34.Guo X, Chen JX, Sun HM, et al, Mining, heterologous expression, purification and characterization of 14 novel bacteriocins from *Lactobacillus rhamnosus* LS-8, *Int. J. Biol. Macromol.*, 164(2020) 2162-2176.https://doi.org/10.1016/j.ijbiomac.2020.08.067.

35.Bertelli C, Tilley KE,Brinkman FSL, Microbial genomic island discovery, visualization and analysis, *Briefings Bioinf.*, 20(2019) 1685-1698.https://doi.org/10.1093/bib/bby042.

36.Joyce SA, MacSharry J, Casey PG, et al, Regulation of host weight gain and lipid metabolism by bacterial bile acid modification in the gut, *PNAS*, 111(2014) 7421-7426.https://doi.org/10.1073/pnas.1323599111.

37.Neumann J, Rose-Sperling D,Hellmich UA, Diverse relations between ABC transporters and lipids: An overview, *Bba-Biomembranes*, 1859(2017) 605-618.https://doi.org/10.1016/j.bbamem.2016.09.023.

38.Zhong SS, Li LX, Liang NN, et al, Acetaldehyde Dehydrogenase 2 regulates HMG-CoA reductase stability and cholesterol synthesis in the liver, *Redox Biol.*, 41(2021).https://doi.org/10191910.1016/j.redox.2021.101919.

39.Lyu Y, Zhong L, Liu Y, et al, Protective effects of Lactococcus lactis expressing alcohol dehydrogenase and acetaldehyde dehydrogenase on acute alcoholic liver injury in mice, *J. Chem. Technol. Biotechnol.*, 93(2018) 1502-1510.https://doi.org/https://doi.org/10.1002/jctb.5521.

40.Zhu K, Ni L, Han J, et al, Acetyl-coenzyme A acetyltransferase 1 promotes brown adipogenesis by activating the AMPK-PGC1α signaling pathway, *BBA-MOL CELL BIOL L*, 1868(2023) 159369.https://doi.org/https://doi.org/10.1016/j.bbalip.2023.159369.

41.Zhou S, Ma N, Meng M, et al, Lentinan Ameliorates β-Hydroxybutyrate-Induced Lipid Metabolism Disorder in Bovine Hepatocytes by Upregulating the Expression of Acetyl-coenzyme A Acetyltransferase 2, *J. Agric. Food. Chem.*, 72(2024) 17392-17404.https://doi.org/10.1021/acs.jafc.4c03279.

42.Zhong S, Li L, Liang N, et al, Acetaldehyde Dehydrogenase 2 regulates HMG-CoA reductase stability and cholesterol synthesis in the liver, *Redox Biol.*, 41(2021) 101919.https://doi.org/10.1016/j.redox.2021.101919.

43.Ambrogi V, Bottacini F, O'Callaghan J, et al, Infant-Associated Bifidobacterial β-Galactosidases and Their Ability to Synthesize Galacto-Oligosaccharides, *Front. Microbiol.*, 12(2021).https://doi.org/10.3389/fmicb.2021.662959.

44.Luo M, Zhou W, Tao W, et al, Whole-Genome Sequencing of *Lactiplantibacillus plantarum* YY-112 and Investigation of Its Immune-Modulating Abilities In Vivo, *Fermentation*, 9(2023).https://doi.org/10.3390/fermentation9120996.

45.Levasseur A, Drula E, Lombard V, et al, Expansion of the enzymatic repertoire of the CAZy database to integrate auxiliary redox enzymes, *Biotechnol Biofuels*, 6(2013) 41.https://doi.org/10.1186/1754-6834-6-41.

46.Tödter D, Gunka K,Stülke J, The Highly Conserved Asp23 Family Protein YqhY Plays a Role in Lipid Biosynthesis in, *Front. Microbiol.*, 8(2017).https://doi.org/88310.3389/fmicb.2017.00883.

47.Li J, Zhu K, Li C, et al, Alkaline shock protein 23 (Asp23)-controlled cell wall imbalance promotes membrane vesicle biogenesis in Staphylococcus aureus, *J. Extracell. Vesicles*, 13(2024) e12501.https://doi.org/https://doi.org/10.1002/jev2.12501.

48.Han M, Liao W, Dong Y, et al, *Lacticaseibacillus rhamnosus* Hao9 exerts antidiabetic effects by regulating gut microbiome, glucagon metabolism, and insulin levels in type 2 diabetic mice, *Front. Nutr.*, 9(2022) 1081778.https://doi.org/10.3389/fnut.2022.1081778.

49.Wang J, Chen J, Gao M, et al, Research Progress on the Mechanism of Action and Screening Methods of Probiotics for Lowering Blood Lipid Levels, *Foods*, 14(2025).https://doi.org/10.3390/foods14091583.

50.Matsuo M, ABCA1 and ABCG1 as potential therapeutic targets for the prevention of atherosclerosis, *J. Pharmacol. Sci.*, 148(2022) 197-203.https://doi.org/https://doi.org/10.1016/j.jphs.2021.11.005.

51.Gil-Rodríguez AM,Beresford T, Bile salt hydrolase and lipase inhibitory activity in reconstituted skim milk fermented with lactic acid bacteria, *J. Funct. Foods*, 77(2021) 104342.https://doi.org/https://doi.org/10.1016/j.jff.2020.104342.

52.Sun YW, Zhang SY, Li H, et al, Assessments of Probiotic Potentials of *Lactiplantibacillus plantarum* Strains Isolated From Chinese Traditional Fermented Food: Phenotypic and Genomic Analysis, *Front. Microbiol.*, 13(2022).https://doi.org/89513210.3389/fmicb.2022.895132.

53.Wang TT, Zhang X, Fan LL, et al, Complete genome sequence and anti-obesity potential of *Lactiplantibacillus plantarum* HOM2217 in 3T3-L1 cells and high-fat diet-fed rats, *Front. Microbiol.*, 15(2024).https://doi.org/143637810.3389/fmicb.2024.1436378.

54.Liu X, Wang M, Hu T, et al, Safety assessment of potential probiotic Lactobacillus acidophilus AM13-1 with high cholesterol-lowering capability isolated from human gut,
Lett. Appl. Microbiol., 77(2024).https://doi.org/10.1093/lambio/ovad143.

55.Liu Q, Lu X, Guo C, et al, The effect of metformin on lipid disorders as measured by nuclear magnetic metabolomics and metabolic flux analysis, *Acta Pharmaceutica Sinica*, 56(2021) 1109-1119.https://doi.org/10.16438/j.0513-4870.2020-1774.

56.Xie X, Geng C, Zhao W, et al, MST1 regulates hepatic gluconeogenesis by promoting PEPCK expression in mice, *Basic & Clinical Medicine*, 40(2020) 1656-1660.https://doi.org/10.16352/j.issn.1001-6325.2020.12.011.

57.Wu CY, Xu DL, Ge M, et al, Blocking glutathione regeneration: Inorganic NADPH oxidase nanozyme catalyst potentiates tumoral ferroptosis, *Nano Today*, 46(2022).https://doi.org/10157410.1016/j.nantod.2022.101574.

58.Kallie E Hays JMP, Rebecca Ryznar, The interplay between gut microbiota, short-chain fatty acids, and implications for host health and disease, *Gut Microbes*, 16(2024).https://doi.org/10.1080/19490976.2024.2393270.

59.Zhao Y, Chen FD, Wu W, et al, GPR43 mediates microbiota metabolite SCFA regulation of antimicrobial peptide expression in intestinal epithelial cells via activation of mTOR and STAT3, *Mucosal Immunol*, 11(2018) 752-762.https://doi.org/10.1038/mi.2017.118.

60.Liu J, Yue S, Yang Z, et al, Oral hydroxysafflor yellow A reduces obesity in mice by modulating the gut microbiota and serum metabolism, *Pharmacol Res*, 134(2018) 40-50.https://doi.org/10.1016/j.phrs.2018.05.012.

61.Feng X, Ding L, Ma G, et al, Lactobacillus rhamnosus TR08 Improves Dyslipidemia in Mice Fed with a High Fat Diet by Regulating the Intestinal Microbiota, Reducing Systemic Inflammatory Response, and Promoting Sphingomholipid Metabolism, *Molecules*, 27(2022) 7357.https://doi.org/10.3390/molecules27217357.

62.Wang YW, Song JL, Zhai Y, et al, *Romboutsia sedimentorum* sp nov., isolated from an alkaline-saline lake sediment and emended description of the genus Romboutsia, *INT J SYST EVOL MICR*, 65(2015) 1193-1198.https://doi.org/10.1099/ijs.0.000079.

63.Huang Y, Li M, Zhou L, et al, Effects of Qingluo Tongbi Decoction on Gut Flora of Rats with Adjuvant-Induced Arthritis and the Underlying Mechanism, *EVID-BASED COMPL ALT* (2019).https://doi.org/10.1155/2019/6308021.

64.Yu YX, Zong ML, Lao LF, et al, Adhesion properties of cell surface proteins in Lactobacillus strains in the GIT environment, *Food Funct.*, 13(2022) 3098-3109.https://doi.org/10.1039/d1fo04328e.

65.MIYOSHI Y, OKADA S, UCHIMURA T, et al, A Mucus Adhesion Promoting Protein, MapA, Mediates the Adhesion of *Lactobacillus reuteri* to Caco-2 Human Intestinal Epithelial Cells, *Biosci. Biotechnol., Biochem.*, 70(2006) 1622-1628.https://doi.org/10.1271/bbb.50688.

66.El-Chami C, Choudhury R, Mohammedsaeed W, et al, Multiple Proteins of *Lacticaseibacillus rhamnosus* GG Are Involved in the Protection of Keratinocytes From the Toxic Effects of *Staphylococcus aureus*, *Front. Microbiol.*, 13(2022).https://doi.org/875542

10.3389/fmicb.2022.875542.

67.Guo YX, Jiang XX, Yang Y, et al, Prevention of necrotizing enterocolitis through surface layer protein of *Lactobacillus acidophilus* CICC6074 reducing intestinal epithelial apoptosis, *J. Funct. Foods*, 47(2018) 91-99.https://doi.org/10.1016/j.jff.2018.05.045.

68.Kadeer G, Fu W, He Y, et al, Effect of different doses of *Lacticaseibacillus paracasei* K56 on body fat and metabolic parameters in adult individuals with obesity: a pilot study, *Nutr. Metab.*, 20(2023) 16.https://doi.org/10.1186/s12986-023-00739-y.